AFRL-RZ-WP-TP-2008-2129

INVESTIGATION OF SEPARATION CONTROL IN LOW PRESSURE TURBINE USING PULSED VORTEX GENERATOR JETS (POSTPRINT)

N. Woods, I. Boxx, R. Sondergaard, M. McQuilling, and M. Wolf

Turbine Branch
Turbine Engine Division

JUNE 2006

AIR FORCE RESEARCH LABORATORY
PROPULSION DIRECTORATE
WRIGHT-PATTERSON AIR FORCE BASE, OH 45433-7251
AIR FORCE MATERIEL COMMAND
UNITED STATES AIR FORCE

REPORT DOCUMENTATION PAGE

Form Approved
OMB No. 0704-0188

1. REPORT DATE *(DD-MM-YY)*	2. REPORT TYPE	3. DATES COVERED *(From - To)*
June 2006	Conference Paper Postprint	01 January 2005 – 01 June 2006

4. TITLE AND SUBTITLE
INVESTIGATION OF SEPARATION CONTROL IN LOW PRESSURE TURBINE USING PULSED VORTEX GENERATOR JETS (POSTPRINT)

5a. CONTRACT NUMBER
In-house

5b. GRANT NUMBER

5c. PROGRAM ELEMENT NUMBER
61102F

6. AUTHOR(S)
N. Woods, I. Boxx, and R. Sondergaard (RZTT)
M. McQuilling and M. Wolf (Wright State University)

5d. PROJECT NUMBER
2307

5e. TASK NUMBER
NP

5f. WORK UNIT NUMBER
2307NP02

7. PERFORMING ORGANIZATION NAME(S) AND ADDRESS(ES)

Turbine Branch (AFRL/RZTT)
Turbine Engine Division
Air Force Research Laboratory, Propulsion Directorate
Wright-Patterson Air Force Base, OH 45433-7251
Air Force Materiel Command, United States Air Force

Wright State University
Department of Mechanical and Materials Engineering
3640 Colonel Glenn Hwy
Dayton, OH 45435-0001

8. PERFORMING ORGANIZATION REPORT NUMBER
AFRL-RZ-WP-TP-2008-2129

9. SPONSORING/MONITORING AGENCY NAME(S) AND ADDRESS(ES)
Air Force Research Laboratory
Propulsion Directorate
Wright-Patterson Air Force Base, OH 45433-7251
Air Force Materiel Command
United States Air Force

10. SPONSORING/MONITORING AGENCY ACRONYM(S)
AFRL/RZTT

11. SPONSORING/MONITORING AGENCY REPORT NUMBER(S)
AFRL-RZ-WP-TP-2008-2129

12. DISTRIBUTION/AVAILABILITY STATEMENT
Approved for public release; distribution unlimited.

13. SUPPLEMENTARY NOTES
Conference paper published in the Proceedings of the AIAA Joint Propulsion Conference (2006), Sacramento, CA. Technical paper contains color. PAO Case Number: WPAFB 08-3355; Clearance date: 22 May 2008.

14. ABSTRACT
The periodic fluctuation of velocity in the boundary layer due to forcing of Vortex Generator Jets (VGJs) injected over the suction surface of the Pack-B turbine blade is reported. Blade Reynolds numbers in the turbine cascade match those that occur in aircraft engines while at high altitude cruise. The blowing ratio, a ratio of the jet velocity to the freestream velocity, was set to 2.The VGJs are pitched at 30° and have a skew angle of 90° to the freestream and are located in two rows at 45% and 63% axial chord. PIV data phase locked to the VGJ forcing was used to obtain planar velocity data around the blade. The phase locked PIV images reveal the fluctuation of the flow velocity in the boundary layer with respect to the pulsing period of the VGJ. This sheds light on the mechanism by which the VGJs suppress laminar separation over the blade suction surface.

15. SUBJECT TERMS
separation control, vortex generator jets, VGJ

16. SECURITY CLASSIFICATION OF:			17. LIMITATION OF ABSTRACT:	18. NUMBER OF PAGES	19a. NAME OF RESPONSIBLE PERSON (Monitor)
a. REPORT	b. ABSTRACT	c. THIS PAGE			Rolf Sondergaard
Unclassified	Unclassified	Unclassified	SAR	20	19b. TELEPHONE NUMBER *(Include Area Code)* N/A

Standard Form 298 (Rev. 8-98)
Prescribed by ANSI Std. Z39-18

Investigation of Separation Control in Low Pressure Turbine Using Pulsed Vortex Generator Jets

N. Woods[*], I. Boxx[**], R. Sondergaard[***]
Air Force Research Laboratory, Propulsion Directorate
Wright Patterson Air Force Base, OH 45433

M. McQuilling[§], M. Wolf[§§]
Department of Mechanical and Materials Engineering
Wright State University
3640 Colonel Glenn Hwy
Dayton, OH 45435-0001

Abstract

The periodic fluctuation of velocity in the boundary layer due to forcing of Vortex Generator Jets (VGJs) injected over the suction surface of the Pack-B turbine blade is reported. Blade Reynolds numbers in the turbine cascade match those that occur in aircraft engines while at high altitude cruise. The blowing ratio, a ratio of the jet velocity to the freestream velocity, was set to 2.The VGJs are pitched at 30^o and have a skew angle of 90^o to the freestream and are located in two rows at 45% and 63% axial chord. PIV data phase locked to the VGJ forcing was used to obtain planar velocity data around the blade. The phase locked PIV images reveal the fluctuation of the flow velocity in the boundary layer with respect to the pulsing period of the VGJ. This sheds light on the mechanism by which the VGJs suppress laminar separation over the blade suction surface.

Nomenclature

B = ratio of mean jet velocity to velocity of cross-flow
t* = cycle time (ranges from 0 to 1)

I. Introduction

Due to low air densities at high altitudes the operating Reynolds number (based on axial chord and inlet velocity) of the low pressure turbine (LPT) in high altitude aircraft can drop well below 25,000. At these low Reynolds numbers the boundary layers on the LPT are largely laminar and thus extremely prone to separation even in the presence of elevated freestream turbulence and wake unsteadiness. This separation occurs on the aft portion of the suction side of the LPT blade. Separation increases the pressure drag on the LPT and causes the overall efficiency of the engine to drop significantly.

Separation on LPTs has been studied extensively. [1]Sharma et al. showed a 300% increase in the pressure loss coefficient at Reynolds number below 95,000. This increase was found to be largely the result of the separation on the trailing 50% of the LPT. [2]Dorney et al. showed numerically and experimentally at two

---

* Graduate Student, AFRL/PRTT, 1950 Fifth St. Bldg 18 WPAFB, OH 45433, Student Member
** Contractor, AFRL/PRTT, 1950 Fifth St. Bldg 18 WPAFB, OH 45433, Member
*** Research Engineer, AFRL/PRTT, 1950 Fifth St. Bldg 18 WPAFB, OH 45433, Senior Member
§ Graduate Student, Wright State College of Engineering and Computer Science, Student Member
§§ Professor, Wright State College of Engineering and Computer Science, Senior Member

different Reynolds numbers (Re=43,000, and Re=86,000) that for the Pack B LPT profile, the flow is separated at 73%C_x. Dorney also computed the separation bubble on the aft portion of the suction surface. This separation bubble was shown to decrease in size with an increase in Reynolds number. [3]Enomoto numerically showed that flow separation near 70%C_x over a LPT at Re=43,556. This is consistent with the research presented by [2]Dorney et al. Enomoto went on to show that at this flow condition the separated flow reattaches at 97%C_x. This separation leads to increase in drag and pressure losses.

Because of significant efficiency penalties that can occur, controlling boundary layer separation on the suction side of the turbine blade is of great importance. There have been a number of methods studied to suppress boundary layer separation, all of which fall into one of two categories. Active control methods, which involve adding energy to the flow by some method, tend to be very effective, but are also complex to implement. They have the benefit that they can be shut off when the control is not needed. Passive flow control methods utilize permanent changes to the geometry of the LPT. They tend to be simple, but less effective, and will affect the flow even at high (non-separating) Reynolds numbers.

Vortex Generator Jets (VGJs) are one method of active separation control which have been studied for many years. [3]Eldrege et al. looked at three cases: a flat plate with no streamwise pressure gradient; a flat plate with a streamwise pressure gradient similar to an LPT suction surface; and flow through a Pack-B cascade. Detailed pressure and velocity measurements showed that vortices produced by the VGJs mix high momentum flow from the freestream with low momentum flow from the boundary layer. This mixing works to suppress separation. Eldrege concluded that steady flow VGJs are efficient at suppressing separation.

[5]Bons et al. looked experimentally at a LPT cascade at three Reynolds numbers (25,000, 50,000, and 100,000) with a single VGJ injection location (63%Cx). They varied the freestream turbulence from 1% to 4% and looked at VGJ blowing ratios – the ratio of per unit area jet to freestream momentum - of 0, 1, 2, and 4. It was shown that a minimum blowing ratio was needed for the jet to penetrate the boundary layer and effect the separation. At lower Reynolds numbers the effect of the steady jet was very dramatic. At higher Reynolds numbers the effect is still present but it is not as dramatic, due to the greatly reduced size of the separation bubble. At very high blowing ratios the momentum deficit was shown to increase. Bons stated the increase in deficit could be due to local separation induced by the injection of the very high momentum jet.

[6]Sondergaard et al. continued the research started by [5]Bons et al. Multiple injection locations (45%C_x, 53%C_x, 63%C_x, 73%C_x, and 83%C_x) were individually studied. A blowing ratio of approximately 2 was shown to be the most effective for all injection locations except 83%C_x which was well behind the mean separation line. Injection at 83%C_x required a blowing ratio of greater than 4 to be effective. Injection locations as far upstream as 25%C_x in front of the separation bubble were shown to be effective. The increase in momentum deficit as shown in [5]Bons et al. was also present at high blowing ratios for certain injection locations.

[7]Bons et al. looked at the effect of pulsing the VGJs at two axial locations (45%C_x and 63%C_x). They showed that for blowing ratios less than 2 the effect of the pulsed VGJ was much larger that that of the steady VGJs. Power Spectral Density plots showed spikes at 10Hz, the pulsing frequency of the jet, throughout the flow. This indicates the pulsed jet influences the flow not just locally, but globally, even beyond the trailing edge of the LPT. It was concluded that Pulsed VGJs control separation and improve the pressure distribution over the blade surface as well as the steady VGJs but with an order of magnitude less mass flow. This is significant because the source for compressed air for VGJs in an operating turbomachine would be bleed air from the compressor stage. Reduced mass flow for the VGJs reduces the cycle impact of their implementation.

[8]Moore studied a superscale VGJ in order to better understand the interaction between the pulsed VGJ and the separated shear layer. He pulsed air at 4Hz through a 2.54cm diameter jet oriented with a pitch angle of 30^o and a skew angle of 90^o on a flat plate - first into quiescent air and then into a separated crossflow. Phase locked velocity measurements were taken using a hot wire anemometer and a particle image velocimetry (PIV) system. Readings were taken in the same plane as the jet. Three duty cycles were examined (50%, 25%, and 10%). Moore showed that a decrease in duty cycle results in a decrease in jet penetration. Although in all cases the starting vortex had time to develop and push away from the jet, Moore showed the starting vortex is only significant for about 3ms after pulsing. He concluded that a duty cycle of as little as 1% could be employed effectively. Results from this work indicated the starting vortex may be responsible for separation control, which is consistent with the result from [7]Bons.

II. Experimental Facility

The linear turbine cascade facility used for this study is described in detail in [6]Sondergaard et al. and [5]Bons et al. so only a brief description will be provided here. The open loop, induction wind tunnel which houses the cascade draws air through the bell-mouth inlet equipped with flow straighteners and conditioners and into the 0.85m tall x 1.22m wide test section at up to 80 m/s (Figure 1). The linear cascade consists of eight 0.88m span by 17.8cm axial chord (C_x) blades fabricated from cast polyurethane. The 2-D blade shape studied is the Pratt & Whitney "Pack-B" research design, which is a Mach number scaled version of a highly loaded LPT blade design. The cascade has a design solidity (axial chord, C_x, divided by blade pitch, S_0) of 1.13, an inlet flow angle of 55 degrees, and a design exit angle of 30 degrees (both angles measured from the plane of the cascade) for a total turning of 95 degrees. Flow velocity uniformity across the baseline eight blade cascade is within ±2% at a Reynolds number of 50,000 with less than 1% freestream turbulence. Inlet velocity and axial chord were chosen as reference quantities for the Reynolds number definition because they are both easily measurable and clearly defined. To convert to a Reynolds number based on true chord, multiply by 1.1. To convert to Reynolds number based on suction side length multiply by 1.46. To convert to Reynolds number based on design exit velocity multiply by 1.64.

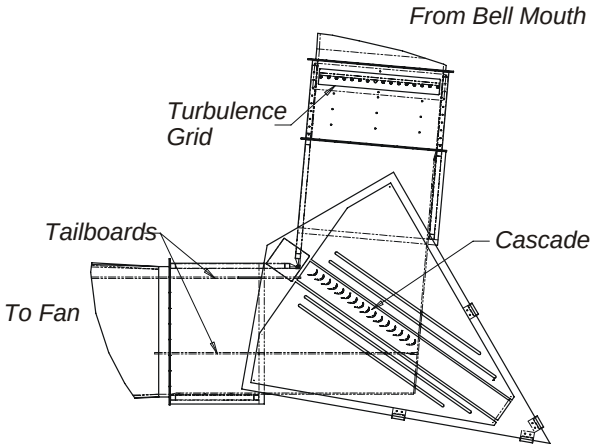

Figure 1: Facility cascade test section.

The blades in the cascade were manufactured with a hollow cavity running all but 5cm of their full span and covering the region from 40% to 90% axial chord (Figure 2). Fittings at the lower end of each blade allow for pressurized feed air for the VGJs and for cavity static pressure measurement. High speed solenoid valves located upstream of the feed ports allow control of the mass flow rate into the blade cavities. Air exhausts from each valve into a short tube that feeds the individual blade cavities. Low bulk massflow rates and the large cavity flow area insure an even distribution of airflow to the individual VGJs. The 0.1cm diameter (d) cylindrical VGJ holes have a 30 degree pitch angle and a 90 degree skew angle. They are spaced every 10d along the center 0.46m of each blade span. For this study, rows of VGJ holes located at 45% and 63% C_x were used.

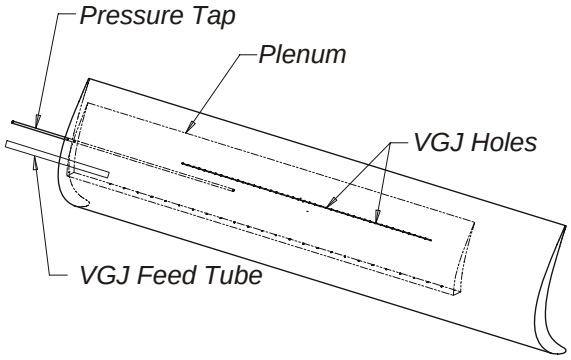

Figure 2: Blade geometry.

To determine the jet blowing ratio, the static pressure in each blade cavity was monitored during tunnel operation. This pressure was corrected for local blade static pressure at the injection location based on the pressure coefficient measured previously for the blade at design pitch and high Reynolds number (Re = 150,000). The resulting driving pressure across the VGJ holes was then correlated to the jet centerline exit velocity using pressure versus velocity data taken earlier outside the cascade tunnel with the jets injecting into stagnant air. Velocity measurements for this correlation were taken approximately 1mm from the VGJ hole exit plane with a sub-miniature hot-film probe prior to installation of the blades in the cascade. The jet blowing ratio, B, was computed as the ratio of the jet exit velocity to the local freestream velocity as calculated from the local pressure coefficient (again using the previously measured values) with the assumption that $\rho_{jet}/\rho_{local} \cong 1$. The primary source of error in the calculation of B is due to the fact that the actual pressure coefficient changes with the amount of flow separation. The effect of this is primarily at the rear of the blade, downstream of the injection locations. Error in the stated blowing ratios is estimated to be less than ±0.3 for all conditions presented.

Instrumentation

Bulk flow instrumentation consisted of flow thermocouples for inlet temperature measurement and an upstream pitot-static reference probe and hotwire to measure inlet conditions. The primary data measurements were made using a phase locked PIV system. The configuration of the PIV system is illustrated in Figure 3. The laser and camera are mounted on a optical breadboard located directly underneath the cascade. The laser is a dual-head, frequency doubled, flashlamp-pumped Nd:YAG laser (New Wave Solo – 120). The laser delivers dual 120 mJ pulses at repetition rates of up to 15Hz. The laser output beam is directed through a high power, adjustable light arm and then through externally mounted sheet forming optics. This produces a light sheet perpendicular to the test blades near the cascade midspan, centered on the middle blade of the cascade.. The flow is seeded with smoke from a theatrical smoke generator placed in front of the wind tunnel's bell mouth inlet. The camera used is a cooled, 14-bit, frame-straddling CCD camera (PCO 1600) with a resolution of 1200 × 1600 pixels and a maximum framing rate of 30 frames per second (fps). The camera images from underneath the test section through the one half inch thick clear plexiglass cascade bottom plate, approximately 50cm from the plane of the light sheet. The camera was fitted with a 105mm lens, which gave a field of view of 163.2mm (cross stream) × 217mm (streamwise).

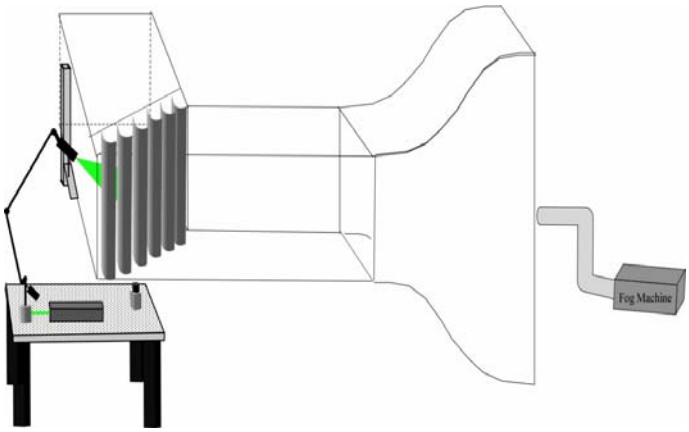

Figure 3: Schematic of Low Speed Wind Tunnel and Particle Image Velocimetry setup used in the current study,

The camera and the laser were phased locked to the trigger of the solenoid valve driving the pulsed vortex generator jets using a digital delay generator. The delay time between the solenoid valve and the PIV system was adjusted to allow data to be taken at different points in the periodic cycle of the VGJs. Images from each data set were stored in the internal memory of the camera and then downloaded to a desktop computer through an IEEE-1394 Firewire™ connection at the end of each run. The images were processed with an adaptive window offset cross-correlation algorithm (Dantec Dynamics Inc. FlowManager v.4.5). The final window size was 32 × 32 pixels with a 50% overlap.

The current study looks at the effect of simultaneously pulsing vortex generator jets located at 45% and 63% C_x on the suction surface of a Pack-B turbine blade. The Reynolds number of the flow was 25,000 based on inlet velocity and axial chord length. The vortex generator jet was pulsed at 10Hz with a duty cycle of 50%. The blowing ratio, ratio of jet mean velocity to freestream velocity, was set to two. The jet was calibrated with a single element hotwire which gave jet velocity as a function of time. This data will be discussed later and presented with phase locked PIV data. Each PIV data set consists of an ensemble average of between 450 and 600 individual image pairs. Each image pair was correlated using the FlowManager software, and the "Peak Validation" option was used to remove errant vectors. The average of the validated, non-substituted vectors was then found using the "Vector Statistics" option. Vorticity data was processed in a similar manner. The ensemble averaged velocity and vorticity data were then exported to Tecplot software for processing and plotting.

III. Results and Discussions

Mean Velocities

Figure 4 shows contour plots of time averaged velocity magnitude over the aft portion of the suction surface of the Pack-B blade at a Reynolds number of 25,000. Figure 4a shows the B=0 (no blowing) case and Figure 4b the B=2 case. Flow is from left to right in each figure. The large separation zone on the rear of the blade shows up clearly as the blue region in Figure 4a. The separated zone is nearly 25mm thick at the rear of the blade. The shear layer between the separation zone and the freestream shows up as green. Since there was no VGJ forcing to phase lock to, the instantaneous structures that exist in the separated layer are washed out by the data averaging. The increase in velocity of the freestream from right to left is due to the acceleration of the flow as it passes through the cascade.

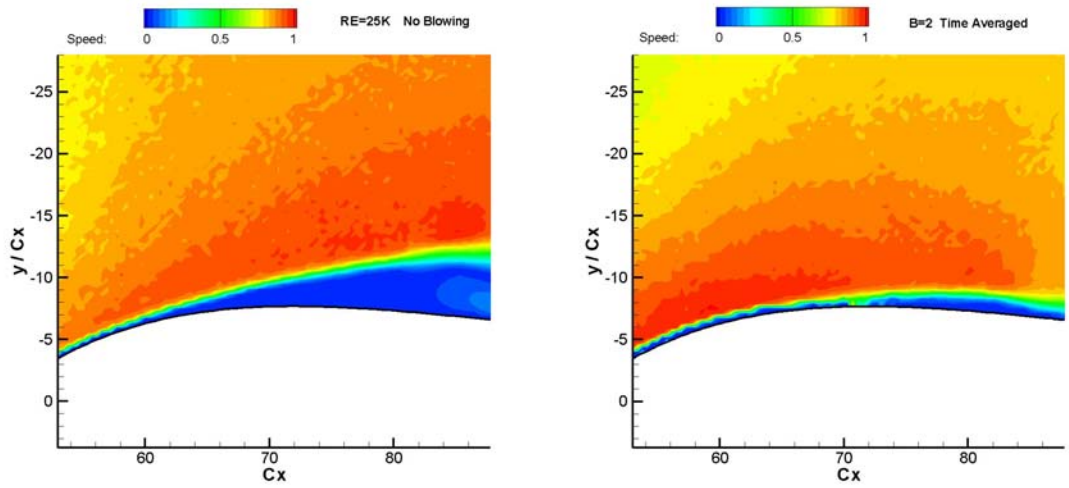

(a) **(b)**

Figure 4. Time average PIV results of Re 25000 for two cases. (a)No blowing. (b) Blowing ratio of 2

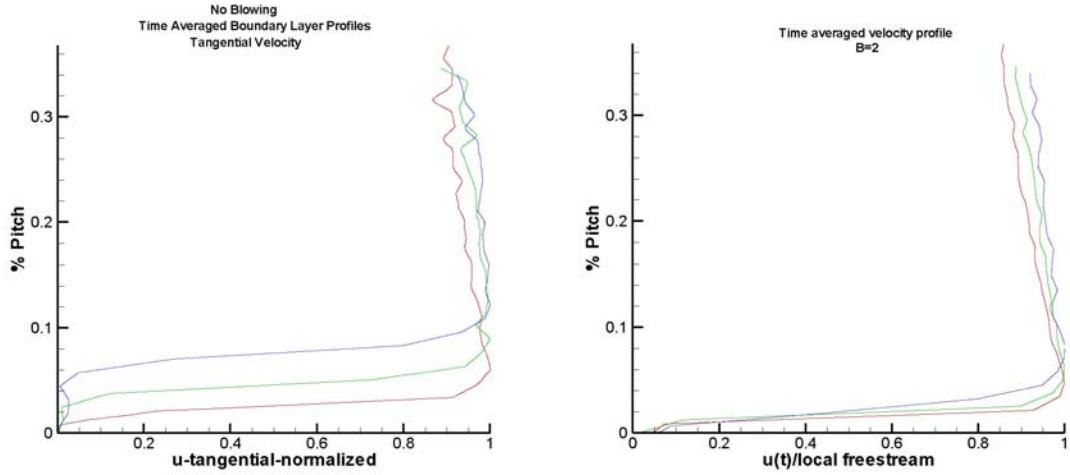

(a) **(b)**

Figure 5. Boundary layer profiles for (a) B=0 and (b) B=2 at 77% (blue), 73% (green), and 68%(red) C_x.

Figure 4b shows an equivalent, time averaged velocity field for the pulsed case. This is not a phase locked, ensemble averaged data set, but a time averaged one, so it shows none of the boundary layer structures generated by the pulsed VGJs. Those structures will be presented later. The 10Hz pulsed VGJs are very effective at suppressing the separation that is so evident in the B=0 case. The pulsed VGJs also causes the maximum freestream velocity to move upstream as compared to the B=0 case. This is because suppressing the separation causes the minimum Cp point to move forward. The jet location on this image is at 0.63 Cx.

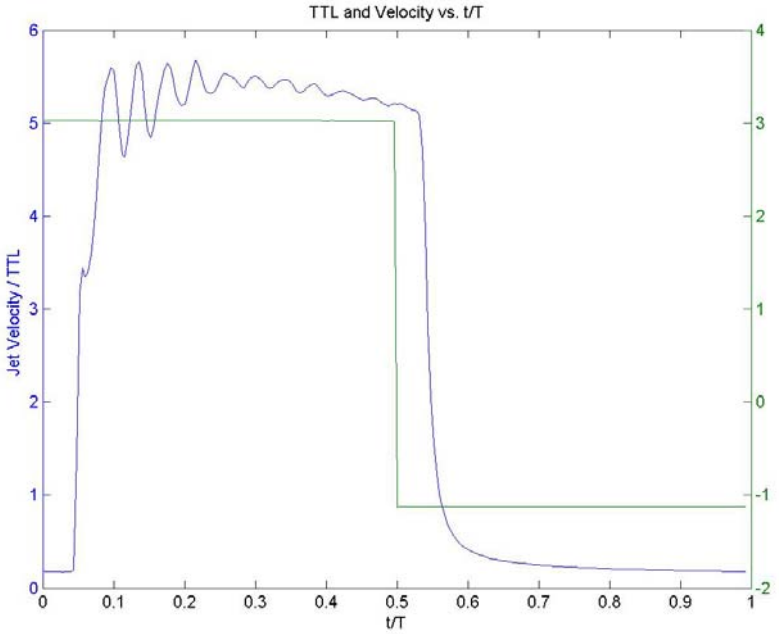

Figure 6. Jet Velocity and the TTL pulse sent the valve shown for one pulsing period with respect to t/T.

Boundary layer profiles extracted from the two time-averaged datasets are shown in Figure 5. The boundary layer profiles have been normalized to the local freestream velocity, and are plots of velocity magnitude, so they do not show reverse flow. The baseline case, with no blowing, shows profiles showing the separated zone at 77%C_x and 73%C_x. The profile at the same locations taken with the B=2 VGJs shows a fully attached boundary layer.

Phase Locked Measurements

Figure 6 shows the response of one of the VGJs to the pulsing of the VGJ feed flow. The TTL pulse sent to the solenoid valve is shown in green and the velocity of air flow exiting the VGJ is shown in red. The valve opens at t* = 0.00. There is a delay of 0.005s after the valve opens before any mass flow exits the VGJ. The rise time of the jet is very small, <0.005s. The velocity reaches a maximum value by about t*=0.1. The exit velocity fluctuates until t*=0.3s due to ringing of the blade feed cavity. At t*=0.5 the valve shuts. Approximately 0.005s later the VGJ velocity begins to fall. The VGJ velocity drops to less than 10% of its peak at t*=0.6 and less than 1% by t* = 0.8.

Figure 7 shows phase (ensemble) averaged velocity magnitude from 54% to 89% Cx of the blade for four phases in the VGJ pulsing cycle, 0^o (solenoid valve opens but no VGJ flow, t*=0), 90^o (jet on, t*=0.25), 180^o (solenoid valve closes, but VGJ flow still on, t*=0.5), & 270^o (valve closed, jet off, t*=0.75). Structures that are phase locked to the VGJ forcing (and therefore related to the forcing) are clearly evident in the boundary layer.

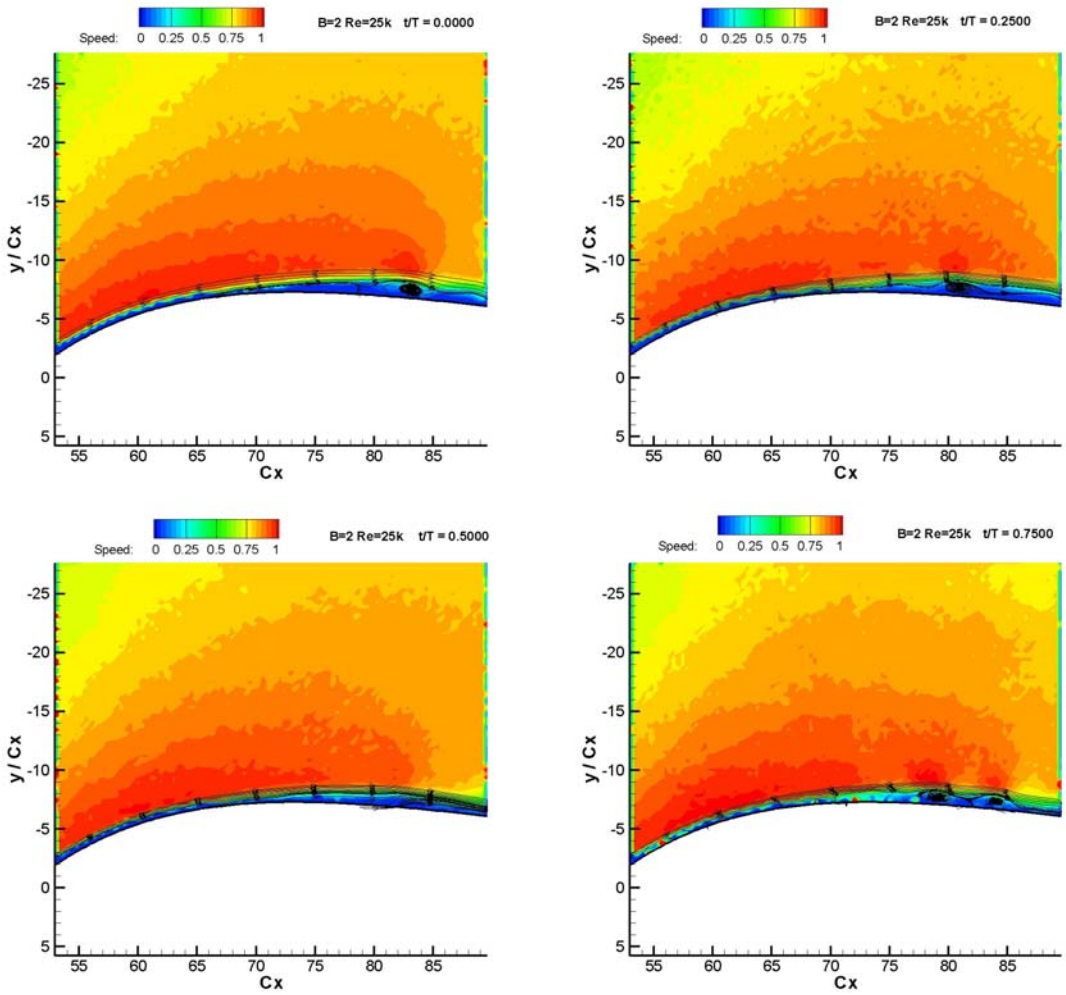

Figure 7: Velocity magnitude with streamlines at 4 points in the pulsing cycle. t* = 0.0000; 0.2500; 0.5000; 0.7500

Figure 8 shows the aft portion of the blade (76% to 89% Cx) in more detail for 32 phases of the VGJ pulsing cycle. Both VGJ injection locations are out of the field of view upstream of these images. Streamlines have been added to help emphasize the flow structures near the blade surface. During the jet pulsing cycle there are at least 8 visible structures that propagate through the measurement region in the boundary layer. The fact that these structures appear in the phase locked, ensemble averaged data implies that they are being driven coherently by the jet pulsing. The coherence of these structures has been verified by examining individual frames of the PIV data (not presented here).

At t*=0.0000 (phase 1) there is a structure which appears to be a boundary layer roller centered at 83% C_x. This and the following phase occurs before any flow exits the VGJs located upstream, and therefore this structure was generated during the previous puling cycle. This structure propagates downstream and can be seen exiting the frame in the next image (t*=0.0313, phase 2) where it is followed by another structure at 77% C_x. Assuming a propagation velocity for the boundary layer rollers of approximately half the freestream velocity (roughly 3% Cx per frame), structures related to the jets turning on would not enter the frame until approximately t* = 0.17, or after phase 6. Therefore this structure must also be related to the previous jet cycle. This structure can be seen propagating downstream through the next five images (t*=0.0625, phase 3, through t*=0.1875, phase 7).

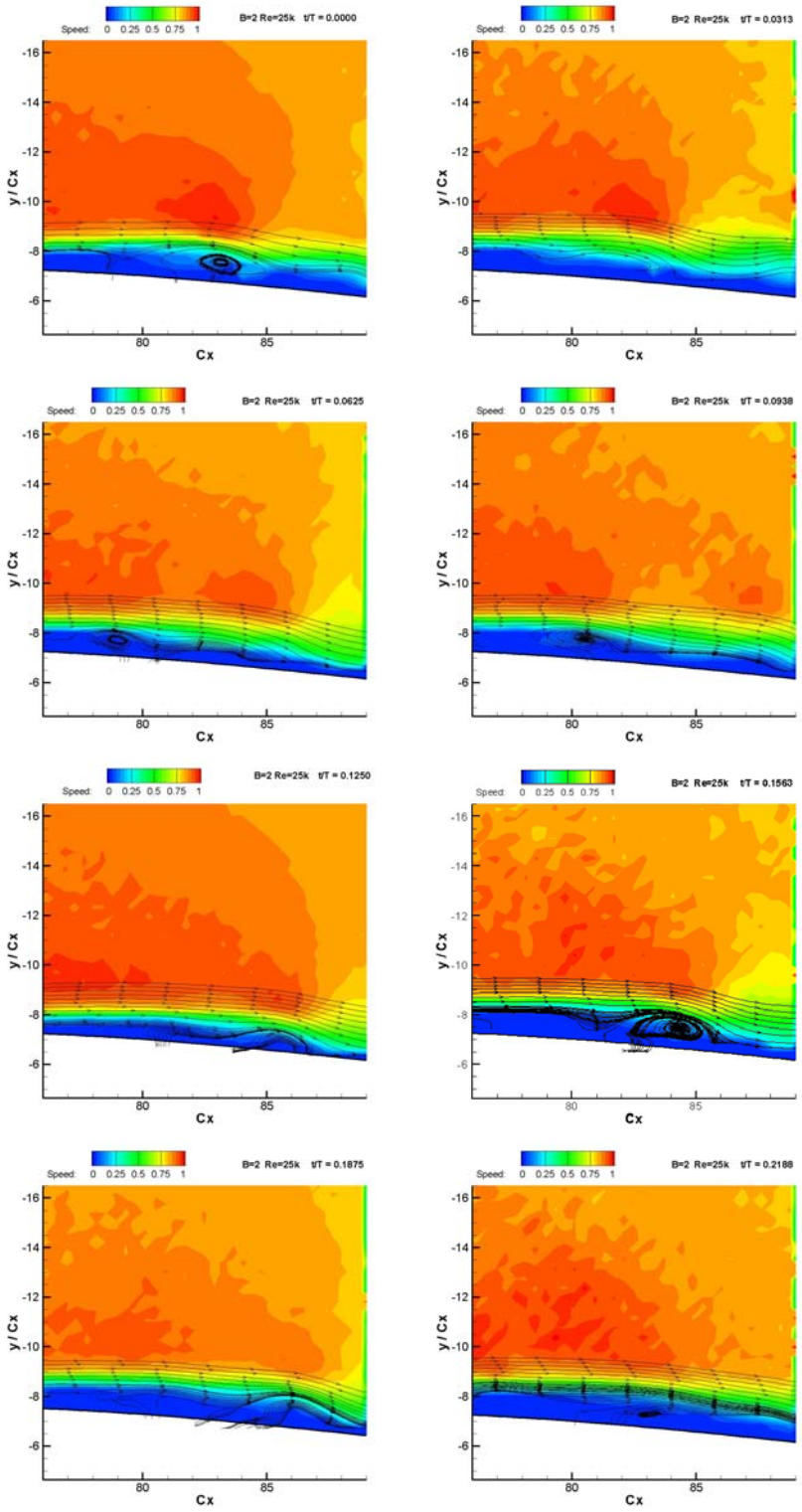
B=2 Re=25k t/T = 0.0000
B=2 Re=25k t/T = 0.0313
B=2 Re=25k t/T = 0.0625
B=2 Re=25k t/T = 0.0938
B=2 Re=25k t/T = 0.1250
B=2 Re=25k t/T = 0.1563
B=2 Re=25k t/T = 0.1875
B=2 Re=25k t/T = 0.2188
Speed: 0 0.25 0.5 0.75 1
y / Cx
Cx
-16
-14
-12
-10
-8
-6
80
85

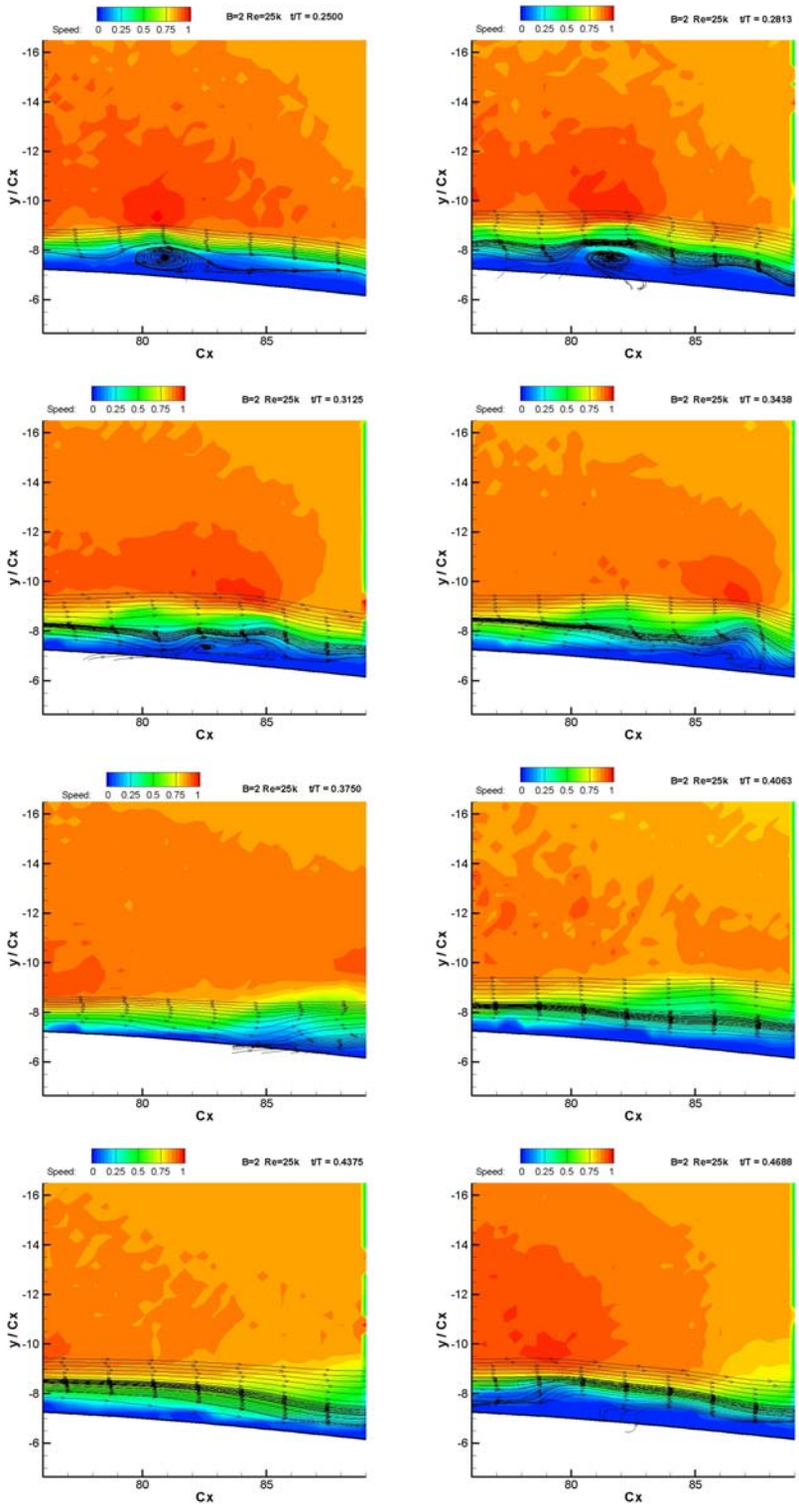
B=2 Re=25k t/T = 0.2500
B=2 Re=25k t/T = 0.2813
B=2 Re=25k t/T = 0.3125
B=2 Re=25k t/T = 0.3438
B=2 Re=25k t/T = 0.3750
B=2 Re=25k t/T = 0.4063
B=2 Re=25k t/T = 0.4375
B=2 Re=25k t/T = 0.4688
Speed: 0 0.25 0.5 0.75 1
y / Cx
Cx
-16
-14
-12
-10
-8
-6
80
85

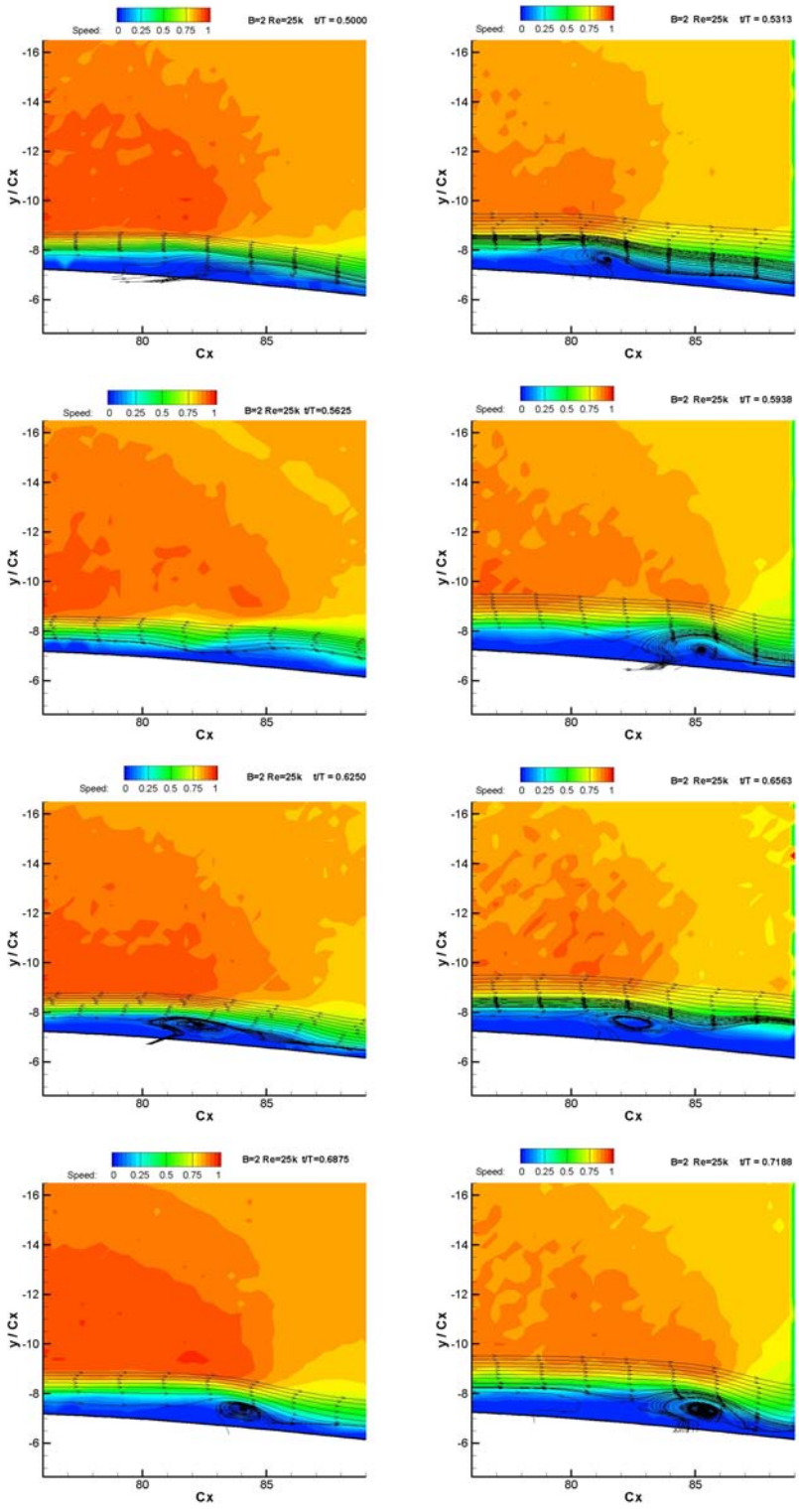
B=2 Re=25k t/T = 0.5000
B=2 Re=25k t/T = 0.5313
B=2 Re=25k t/T=0.5625
B=2 Re=25k t/T = 0.5938
B=2 Re=25k t/T = 0.6250
B=2 Re=25k t/T = 0.6563
B=2 Re=25k t/T=0.6875
B=2 Re=25k t/T = 0.7188
Speed: 0 0.25 0.5 0.75 1
y / Cx
Cx
-16
-14
-12
-10
-8
-6
80
85

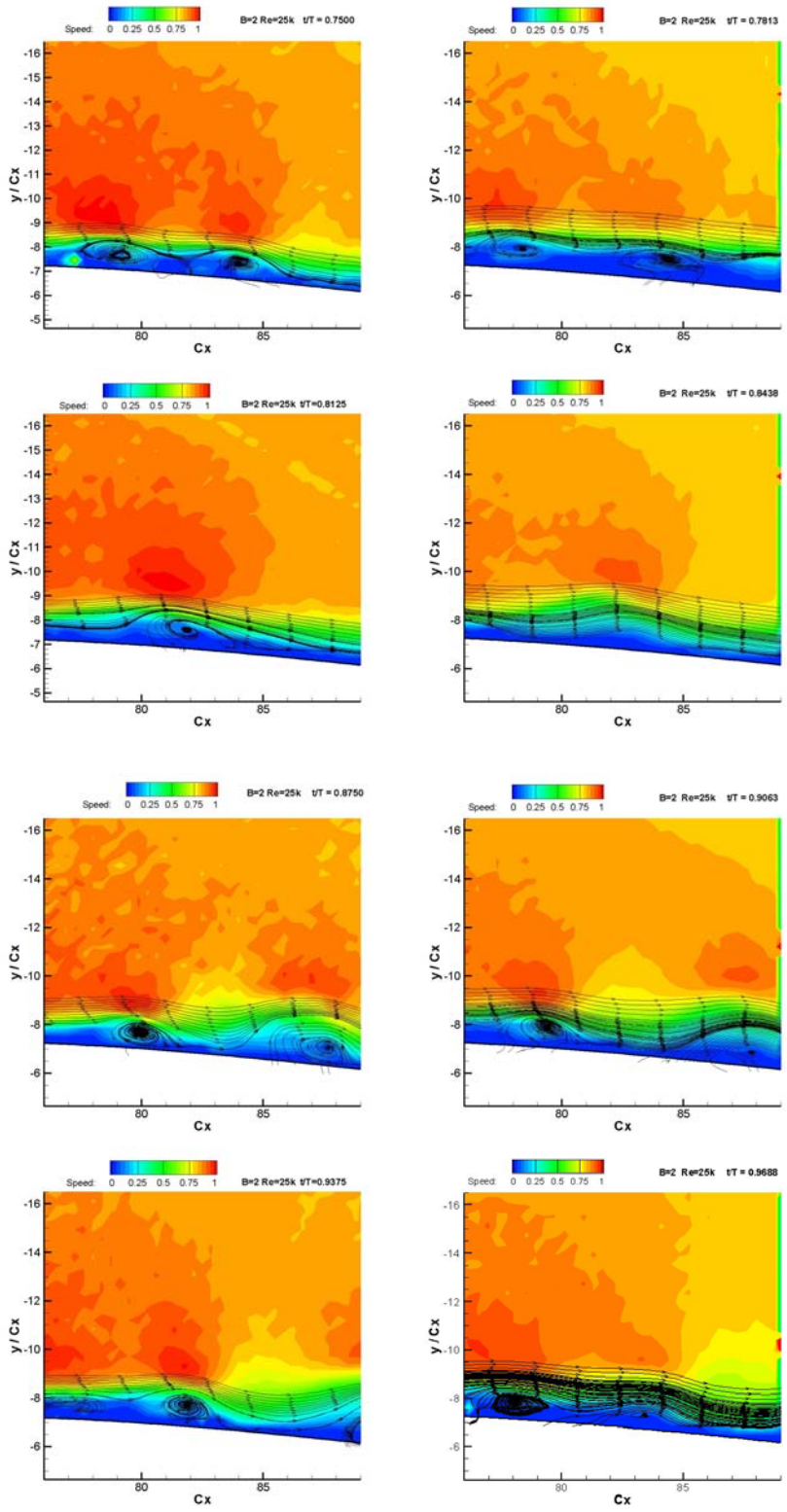

Figure 8:
Velocity Contour with streamlines of the aft portion (76%-89%C_x) of the suction surface of a Pack-B

At t*=0.2188 (phase 8) the boundary layer appears quiescent, though there may be a hint of the structure which appears more coherently in next five images (t* = 0.2500, phase 9 through t* = 0.3750, phase 13). This is the first structure in the boundary layer that can reasonably be assumed to be related to the VGJs turning on. Somewhat surprisingly this does not appear to be a particularly strong or coherent roller as one would expect if the VGJs were seriously disrupting the boundary layer upstream. Another quiescent period follows for the next 4 phases, though there is a sign of the structure that appears more clearly in phases 18 (t* = 0.5313) through 20 (t* = 0.5938). The fact that this structure appears clearly in frames 18 and 20 but much more blurred in the other frames indicates its phase locking to the jet pulsing is not perfect. Note that the valves feeding the VGJs shuts off at t* = 0.5000 (frame 17) thought the VGJs flow doesn't stop until after frame 18 (at approximately t* = 0.55 – see Figure 6). Again the effect of the VGJ shutoff shouldn't arrive at the imaged region until roughly t* = 0.66, after phase 22.

After the VGJs shut off, and the effect has time to convect downstream, there is an increase in the activity seen in the boundary layer. Phases 24 (t* = 0.7188) through 32 (t* = 0.9688) all have two coherent, and rather strong rollers convecting through the frame at any given time. Note that none of these structures can be reasonably linked to the "ringing" seen in the VGJ flow in Figure 6. The ringing occurs at a frequency of approximately 250Hz while the visible structures have a frequency of roughly 80Hz.

Because of the relative weak activity in the boundary layer when the VGJs are on and the increase in frequency and strength of structures in the boundary layer when the VGJs are off, it appears that the VGJs, when on, tend to disrupt, but not completely eliminate the development of the spanwise instabilities in the boundary layer that lead eventually to the development of flow separation. Interestingly it appears there is a period after the VGJ shuts off during which the spanwise instabilities begin to develop, but during which they remain phase-locked to the VGJ pulsing.. This forcing of the instabilities may serve to limit their growth. Thus even if the duty cycle of the VGJ is very short, significant suppression of the spanwise rollup can occur. This is consistent with the studies of [7]Bons et al. who showed that pulsed VGJ duty cycles down to 1% were still effective.

IV. Conclusions

The primary mechanism for the suppression of separation by vortex generator jets on a low pressure turbine blade appears to be the reduction of the spanwise instabilities in the blade boundary layer. When the VGJs are off, spanwise instabilities develop more rapidly and eventually lead to the development of a full blown separation zone. The VGJs disrupt the growth of these spanwise instabilities, suppressing and breaking up the spanwise rollers, and eliminating the resulting separation.

At least eight separate flow structures were seen during the course of one VGJ pulsing cycle, hence the structures are forming with a frequency of approximately 80Hz. The jets are pulsed at 10Hz and ring at about 250 Hz at the beginning of the pulse. The source of the 80Hz forcing is unclear, though it is in the observed range for the unsteady boundary layer separation on the uncontrolled blade. There is also the question of why the 80Hz instability is phase locked to the 10Hz forcing. More tests, at a high phase and space resolution are required for more conclusive data. It is clear however that with the VGJ off the flow structures developed at a higher frequency and seemed to be stronger than when the VGJs were on.

Pulsing the VGJs still results in effective separation suppression because there is a time lag between the ending of the VGJ jet flow and the growth of the spanwise instabilities. As long as the VGJ pulsing period is short enough that each subsequent pulse occurs before the spanwise instability in the boundary layer has grown significantly, separation will, in the mean, be suppressed.

VI. References

[1]Sharma et al. 1998, private communication

[2]Dorney, D., Lake J., King P., Ashpis D., "Experimental and Numerical Investigation of Losses in Low Pressure Turbine Blade Rows", AIAA 2000-0737, January 2000

[3]Enomoto, S., Hah, C., Loellbach, J., "Numerical Investigation of a Low Reynolds Number Flow Field on a Turbine Blade Row", AIAA 2001-0524, January 2001

[4]Eldrege, R., Bons J., "Control of A Separating Boundary Layer with Steady Vortex Generating Jets – Detailed Flow Measurements", AIAA 2004-0751, January 2004

[5]Bons, J., Sondergaard, R., Rivir, R., "Control of Low Pressure Turbine Separation Using Vortex Generator Jets", AIAA-99-0367, January 1999

[6]Sondergaard, R., Rivir, R., Bons, J., "Control of Low Pressure Turbine Separation Using Vortex Generator Jets", Journal of Propulsion and Power

[7]Bons, J. , Sondergaard, R. ,Rivir, R. "Turbine Separation Control Using Pulsed Vortex Generator Jets", ASME 2000-GT-0262, 2000.

[8]Moore, K., Wolff M., "Large Scale Visualization of Pulsed Vortex Generator Jets", AiAA 2005-0346, January 2005

[9]Moore, K. , Wolff, M. , Polanka M. , Sondargaard, R. , "A PIV Study of Pulsed Vortex Generator Jets" , AIAA 2004-3927, July 2004

[10]McQuilling, M., Jacob, J., "A Comparative Study Between Ejector Nozzle and Vortex Generator Jet Flow Control Methods on al Low Pressure Turbine Blade Cascade Model", AIAA 2003-4159, June 2003

[11]McQuilling, M., Hollon, B., Jacob J., "Active Separation Flow Control in a Low Pressure Turbine Blade Cascade Model", AIAA 2003-0615, January 2003

[12]Rivir, R. , Sondergaard, R. , Bons, J. , Yurchenko N. , "Control of Separation in Turbine Boundary Layers", AIAA 2004-2201, July 2004